Evaluation of Group 4 Metal Bis-cyclopentadienyl Complexes with Selenolate and Tellurolate Ligands for CVD of ME_2 Films (E = Se or Te)

Andrew L. Hector, William Levason, Gillian Reid,* Stuart D. Reid, and Michael Webster

School of Chemistry, University of Southampton, Southampton SO17 1BJ, United Kingdom

Received March 19, 2008. Revised Manuscript Received May 12, 2008

The selenolate and tellurolate complexes $[Cp_2M(SeR)_2]$ (M = Ti, Zr, or Hf; R = Me or Bu^t) and $[Cp_2M(TeBu^t)_2]$ (M = Zr or Hf) have been prepared and characterized by ^1H, $^{13}C\{^1H\}$, $^{77}Se\{^1H\}$ and $^{125}Te\{^1H\}$ NMR spectroscopy and microanalysis. Crystal structures of representative examples are reported, together with the structure of the oxo-bridged species $[\{Cp_2Zr(SeMe)\}_2(\mu\text{-}O)]$ formed by partial hydrolysis. Trends in the NMR parameters are discussed. These molecular $[Cp_2M(SeBu^t)_2]$ complexes are shown to be suitable as precursors for the single source LPCVD of intensely colored MSe_2 thin films for each of the Group 4 elements, confirmed by SEM/EDX and PXD. These are the first examples of single source CVD of $ZrSe_2$ and $HfSe_2$ thin films. The corresponding $[Cp_2M(TeBu^t)_2]$ species (M = Zr or Hf) deposit elemental Te under similar LPCVD conditions.

Introduction

Early transition metal chalcogenides, ME_2 (E = S, Se, Te), continue to attract considerable interest owing to their applications as cathode materials for rechargeable batteries,[1] high temperature lubricants,[2] photoelectronics, and gas sensors.[3] In the simplest case, such materials adopt the layered CdI_2 structure, and a series of other structure types are achieved by varying the way that the E−M−E layers stack. By careful selection of the metal and chalcogen, the band gap of the material can be tuned. Thus, for the Group IV cations the indirect band gap increases from 0.2 eV for TiS_2 to 1.96 eV for HfS_2 due to the increase in electropositivity down the Group, while a reduction in band gap is observed on decreasing electronegativity of the chalcogen ($TiSe_2$ = 0.1 eV and $HfSe_2$ = 1.13 eV).[4]

There are a variety of routes to the CVD (chemical vapor deposition) of TiS_2 films,[5] although each preparation generally requires a reactive sulfur group or thiolate. For example, dual source APCVD (atmospheric pressure CVD) using $TiCl_4$ or $Ti(NMe_2)_4$ with a range of thiols or thiolates; AACVD (aerosol assisted CVD) using $Ti(NMe_2)_4$ and RSH or $S_2Bu^t_2$; and single source LPCVD (low pressure CVD) using $[TiCl_4(RSH)_2]$.[6–8] Recently, we demonstrated that LPCVD with the single source precursor $[TiCl_4\{o\text{-}C_6H_4(CH_2SMe)_2\}]$ leads to deposition of TiS_2—a very rare example of early transition metal sulfide formation from a precursor involving a neutral thioether ligand.[9] In contrast, the only reported single source CVD routes to $TiSe_2$ films are from LPCVD of $[TiCl_4(SeEt_2)_2]$[10] and $[TiCl_4\{o\text{-}C_6H_4(CH_2SeMe)_2\}]$.[9]

The formation of the heavier Group 4 selenides, $ZrSe_2$ and $HfSe_2$, has been limited to the reactions of the constituent elements followed by purification by chemical transport reactions using I_2 as a transport agent.[11] There have been no examples of deposition of these materials by CVD methods. We report here the syntheses, characterization, and structures of a series of bis-cyclopentadienyl chalcogenolate complexes of Ti, Zr, and Hf and describe the results of our investigations of their use as single source precursors for the deposition of ME_2 thin films.

A number of selenolate and fewer tellurolate complexes of the form $[Cp_2M(ER)_2]$ (M = Ti, Zr, Hf; E = Se, Te) have been reported previously, although mainly with R = Ph or bulky silyl groups.[12] There are no examples of these species being used as CVD precursors, although LPCVD of

* Corresponding author. E-mail: gr@soton.ac.uk. Fax: 023 80593781.

(1) Gabane, J. P. *Lithium Batteries*: Academic Press: London, 1983.
(2) McTaggart, F. K.; Moore, A. *Aust. J. Chem.* **1958**, *11*, 481–484.
(3) (a) Pathak, V. M.; Patel, K. D.; Pathak, R. J.; Srivastava, R. *Sol. Energy Mater. Sol. Cells* **2002**, *73*, 117–123. (b) Kishiro, K.; Takemoto, S.; Kuriyaki, H.; Hirakawa, K. *Jpn. J. Appl. Phys.* **1994**, *33*, 1069–1073.
(4) Hoffmann, R. *Solids and Surfaces: A Chemist's View of Bonding in Extended Structures*; VCH: Weinheim, 1988.
(5) Palgrave, R. G.; Parkin, I. P. *New J. Chem.* **2006**, *30*, 505–514.
(6) (a) Winter, C. H.; Lewkebandara, T. S.; Proscia, J. W. *Chem. Mater.* **1992**, *4*, 1144–1146. (b) Carmalt, C. J.; Dinnage, C. W.; Parkin, I. P.; Peters, E. S.; Molloy, K.; Colucci, M. A. *Polyhedron* **2003**, *22*, 1255–1262. (c) Carmalt, C. J.; Parkin, I. P.; Peters, E. S. *Polyhedron* **2003**, *22*, 1263–1269.
(7) Peters, E. S.; Carmalt, C. J.; Parkin, I. P. *J. Mater. Chem.* **2004**, *14*, 3474–3477.
(8) Winter, C. H.; Lewkebandara, T. S.; Proscia, J. W.; Rheingold, A. L. *Inorg. Chem.* **1993**, *32*, 3807–3808.
(9) Reid, S. D.; Hector, A. L.; Levason, W.; Reid, G.; Waller, B. J.; Webster, M. *Dalton Trans.* **2007**, 4769–4777.
(10) McKarns, P. J.; Lewkebandara, T. S.; Yap, G. P. A.; Liable-Sands, L. M.; Rheingold, A. L.; Winter, C. H. *Inorg. Chem.* **1998**, *37*, 418–424.
(11) (a) Amberg, M.; Günter, J. R. *Solid State Ionics* **1996**, *84*, 313–321. (b) Zheng, X.-G.; Kuriyaki, H.; Hirakawa, K. *J. Phys. Soc. Jpn.* **1989**, *58*, 622–626.
(12) Arnold, J. *Prog. Inorg. Chem.* **1995**, *43*, 353–417, and references therein.

10.1021/cm800802g CCC: $40.75
Published on Web 07/02/2008

$[Cp_2Ti(SBu^t)_2]$ and $[Cp_2Zr(SBu^t)_2]$ gave films of apparent stoichiometry $TiS_{1.3}$ and ZrS, respectively.[13]

Experimental Section

^1H and $^{13}C\{^1H\}$ NMR spectra were recorded using a Bruker AV300 spectrometer operating at 300.1 and 75.5 MHz, respectively, and are referenced to TMS. $^{77}Se\{^1H\}$ and $^{125}Te\{^1H\}$ NMR spectra were recorded using a Bruker DPX400 spectrometer operating at 100.6 or 126.4 MHz, respectively, and are referenced to external neat Me_2Se or Me_2Te. Microanalyses were undertaken by the University of Strathclyde or the Medac microanalytical service.

Solvents were dried by distillation from CaH_2 (CH_2Cl_2) or sodium (toluene, hexane) prior to use, and all preparations were undertaken using Schlenk and vacuum line techniques with flame dried glassware under a dry N_2 atmosphere. Celite was dried before use by heating in vacuo. All solid samples were handled in a glovebox (<1 ppm water). Yields quoted are based upon the first crop of crystalline material isolated from the reactions and used for the depositions. Further material could be obtained by addition of hexane to the mother liquor, giving total yields of around 60%. $[Cp_2MCl_2]$ (M = Ti, Zr or Hf) were obtained from Aldrich and used as received.

Precursor Synthesis. *$[Cp_2Ti(SeMe)_2]$.* To a frozen (77 K) suspension of Se powder (549 mg, 6.96 mmol) in THF (10 mL) was added dropwise LiMe (5 mL, 1.6 M in Et_2O). Upon warming to room temperature the solids dissolved to give a colorless solution. After a further 1 h of stirring, the resulting Li salt was added to a stirred suspension of $[Cp_2TiCl_2]$ (866 mg, 3.48 mmol) in toluene (10 mL) to give a green solution which was stirred at room temperature overnight. The volatiles were removed at reduced pressure and the green solid extracted with CH_2Cl_2 (15 mL) and filtered through celite. The precipitate was washed with CH_2Cl_2 (3 × 10 mL), and the CH_2Cl_2 washings were combined and concentrated, approximately 10 mL. Green crystals of $[Cp_2Ti(SeMe)_2]$ were obtained by decanting. Yield: 253 mg, 20%. Anal. Calcd for $C_{12}H_{16}Se_2Ti$ (366.04): C, 39.37; H, 4.41. Found: C, 39.58; H 4.02%. ^1H NMR (CD_2Cl_2, 300 K): δ_H = 6.13 (s, 10H, Cp), 2.73 (s, 6H, Me). $^{13}C\{^1H\}$ NMR (CD_2Cl_2, 300 K): δ_C = 110.8 (s, Cp), 14.3 (s, Me). $^{77}Se\{^1H\}$ NMR (CH_2Cl_2/$CDCl_3$, 300 K): δ_{Se} = 914.2.

$[Cp_2Zr(SeMe)_2]$. Was made similarly to the above and isolated as pale yellow crystals. Yield: 18%. Anal. Calcd for $C_{12}H_{16}Se_2Zr$ (409.40): C, 35.20; H, 3.94. Found: C, 34.92; H, 3.95%. ^1H NMR (CD_2Cl_2, 300 K): δ_H = 6.18 (s, 10H, Cp), 2.38 (s, 6H, Me). $^{13}C\{^1H\}$ NMR (CD_2Cl_2, 300 K): δ_C = 110.0 (s, Cp), 7.8 (s, Me). $^{77}Se\{^1H\}$ NMR (CH_2Cl_2/$CDCl_3$, 300 K): δ_{Se} = 449.5.

$[\{Cp_2Zr(SeMe)\}_2(\mu\text{-}O)]$. Exposure of a solution of $[Cp_2Zr(SeMe)_2]$ prepared as above to moist CH_2Cl_2 led to hydrolysis and the isolation of $[\{Cp_2Zr(SeMe)\}_2(\mu\text{-}O)]$. Yield: 17%. Anal. Calcd for $C_{22}H_{26}OSe_2Zr_2$ (646.81): C, 40.85; H, 4.05. Found: C, 40.45; H, 4.06%. ^1H NMR (CD_2Cl_2, 300 K): δ_H = 6.14 (s, 10H, Cp), 2.38 (s, 3H, Me). $^{13}C\{^1H\}$ NMR (CD_2Cl_2, 300 K): δ_C = 111.7 (s, Cp), 3.5 (s, CH_3). $^{77}Se\{^1H\}$ NMR (CH_2Cl_2/CD_2Cl_2, 300 K): δ_{Se} = 192.0.

$[Cp_2Hf(SeMe)_2]$. This was made similarly to the $[Cp_2Ti(SeMe)_2]$ described above and isolated as pale yellow crystals. Yield: 28%. Anal. Calcd for $C_{12}H_{16}HfSe_2$ (496.67): C, 29.02; H, 3.25. Found: C, 29.06; H, 3.33%. ^1H NMR (CD_2Cl_2, 300 K): δ_H = 6.12 (s, 10H, Cp), 2.47 (s, 6H, Me). $^{13}C\{^1H\}$ NMR (CD_2Cl_2, 300 K): δ_C = 109.0 (s, Cp), 7.5 (s, CH_3). $^{77}Se\{^1H\}$ NMR (CH_2Cl_2/CD_2Cl_2, 300 K): δ_{Se} = 311.1.

$[Cp_2Ti(SeBu^t)_2]$. To a frozen (77 K) suspension of Se powder (1.90 g, 24.1 mmol) in THF (50 mL) was added dropwise $LiBu^t$ (21 mL, 1.7 M in pentane). Upon warming to room temperature the solids dissolved to give a yellow solution. After a further 1 h of stirring, the resulting Li salt was added to a stirred suspension of $[Cp_2TiCl_2]$ (3.00 g, 12.0 mmol) in toluene (50 mL) to give a green solution which was stirred at room temperature overnight. The volatiles were removed at reduced pressure, and the resulting green solid was extracted with Et_2O (100 mL) and filtered through celite. The residual solids were washed with Et_2O (3 × 25 mL), all Et_2O washings were combined, and the volume was reduced in vacuo. The liquors were cooled, and $[Cp_2Ti(SeBu^t)_2]$ was isolated as green crystals by decanting and finally drying in vacuo. Yield: 1.46 g, 27%. Anal. Calcd for $C_{18}H_{28}Se_2Ti$ (450.20): C, 48.02; H, 6.27. Found: C, 47.65; H, 6.27%. ^1H NMR (CD_2Cl_2, 300 K): δ_H = 6.19 (s, 10H, Cp), 1.62 (s, 18H, Bu^t). $^{13}C\{^1H\}$ NMR (CD_2Cl_2, 300 K): δ_C = 110.6 (s, Cp), 42.7 (s, C_q), 36.2 (s, CMe_3). $^{77}Se\{^1H\}$ NMR (CH_2Cl_2/CD_2Cl_2, 300 K): δ_{Se} = 1272.4.

$[Cp_2Zr(SeBu^t)_2]$. This was made similarly to the previous compound and isolated as yellow crystals. Yield: 23%. Anal. Calcd for $C_{18}H_{28}Se_2Zr$ (493.56): C, 43.80; H, 5.72. Found: C, 43.76; H, 5.76%. ^1H NMR ($CDCl_3$, 300 K): δ_H = 6.24 (s, 10H, Cp), 1.65 (s, 18H, Bu^t). $^{13}C\{^1H\}$ NMR (CD_2Cl_2, 300 K): δ_C = 109.8 (s, Cp), 41.9 (s, C_q), 36.7 (s, CMe_3). $^{77}Se\{^1H\}$ NMR (CH_2Cl_2/CD_2Cl_2, 300 K): δ_{Se} = 841.5.

$[Cp_2Hf(SeBu^t)_2]$. This was made similarly and isolated as pale yellow crystals. Yield: 64%. Anal. Calcd for $C_{18}H_{28}HfSe_2$ (580.82): C, 37.22; H, 4.86. Found: C, 37.13; H, 4.91%. ^1H NMR ($CDCl_3$, 300 K): δ_H = 6.18 (s, 10H, Cp), 1.66 (s, 18H, Bu^t). $^{13}C\{^1H\}$ NMR ($CDCl_3$, 300 K): δ_C = 108.7 (s, Cp), 36.8 (s, CMe_3), quaternary carbon not observed. $^{77}Se\{^1H\}$ NMR (CH_2Cl_2/CD_2Cl_2, 300 K): δ_{Se} = 669.0.

$[Cp_2Zr(TeBu^t)_2]$. To a frozen (77 K) suspension of freshly ground Te (260 mg, 2.04 mmol) in THF (15 mL) was added dropwise $LiBu^t$ (1.8 mL, 1.7 M in pentane). Upon warming to room temperature the solids dissolved to give a yellow solution. After a further 15 min of stirring, the resulting Li salt was cooled to −78 °C and added dropwise to a cold (−78 °C) stirred suspension of $[Cp_2ZrCl_2]$ (300 mg, 1.02 mmol) in toluene (15 mL) to give a purple solution which was stirred for 2 h. The volatiles were then removed at reduced pressure and the purple solid extracted with Et_2O (20 mL) and filtered through celite. The precipitate was washed with Et_2O (2 × 15 mL), all the Et_2O washings were combined, and the solvent volume was reduced to approximately 10 mL. Upon cooling, purple crystals were isolated by decanting. Yield: 74 mg, 12%. ^1H NMR ($CDCl_3$, 300 K): δ_H = 6.13 (s, 10H, Cp), 1.71 (s, 18H, Bu^t). $^{13}C\{^1H\}$ NMR ($CDCl_3$, 300 K): δ_C = 107.9 (s, Cp), 39.9 (s, CMe_3), 21.9 (s, Cq). $^{125}Te\{^1H\}$ NMR (CH_2Cl_2/$CDCl_3$, 300 K): δ_{Te} = 1204.7.

$[Cp_2Hf(TeBu^t)_2]$. This was made similarly and isolated as orange crystals. Yield: 23%. ^1H NMR ($CDCl_3$, 300 K): δ_H = 6.05 (s, 10H, Cp), 1.72 (s, 18H, Bu^t). $^{13}C\{^1H\}$ NMR ($CDCl_3$, 300 K): δ_C = 106.6 (s, Cp), 39.6 (s, CMe_3), 22.3 (s, C_q). $^{125}Te\{^1H\}$ NMR (CH_2Cl_2/$CDCl_3$, 300 K): δ_{Te} = 976.1.

X-ray Crystallography. Crystals were obtained as described in the text. Data collection used a Nonius Kappa CCD diffractometer with monochromated (confocal mirror or graphite) Mo Kα X-ray radiation (λ = 0.71073 Å) with the crystal held at 120 K in a cooled nitrogen gas stream. Structure solution and refinement were straightforward[14,15] with H atoms introduced into the model in

(13) Senocq, F.; Viguier, H.; Gleizes, A. *Eur. J. Solid State Inorg. Chem.* **1996**, 1185–1197.

(14) Sheldrick, G. M. *SHELXS-97, program for crystal structure solution*; University of Göttingen: Göttingen, Germany, 1997.

(15) Sheldrick, G. M. *SHELXL-97, program for crystal structure refinement*; University of Göttingen: Göttingen, Germany, 1997.

Table 1. $^{77}Se\{^1H\}$ and $^{125}Te\{^1H\}$ NMR Spectroscopic Data[a]

compound	$\delta(^{77}Se)$ or $\delta(^{125}Te)$, ppm	Δ, ppm[b,c]
$[Cp_2Ti(SeMe)_2]$	914.2	1260.2
$[Cp_2Zr(SeMe)_2]$	449.5	795.5
$[Cp_2Hf(SeMe)_2]$	311.1	657.1
$[Cp_2Ti(SeBu^t)_2]$	1272.4	1100.3
$[Cp_2Zr(SeBu^t)_2]$	841.5	669.4
$[Cp_2Hf(SeBu^t)_2]$	669.0	496.9
$[Cp_2Zr(TeBu^t)_2]$	1204.7	1109.4
$[Cp_2Hf(TeBu^t)_2]$	976.1	880.8

[a] Data recorded at 300 K from CD_2Cl_2/CH_2Cl_2 solutions of the complexes. [b] $\Delta = [\delta(Cp_2M(ER)_2) - \delta(LiER)]$. [c] LiSeMe in THF solution: $\delta(^{77}Se\{^1H\}) = -346.0$. $LiSeBu^t$ in THF solution: $\delta(^{77}Se\{^1H\}) = 172.1$. $LiTeBu^t$ in THF solution: $\delta(^{125}Te\{^1H\}) = 95.3$.

Table 2. Selected Bond Lengths [Å] and Angles [deg] for $[Cp_2Ti(SeMe)_2]$

Ti1−C1	2.404(5)	Ti1−C2	2.361(5)
Ti1−C3	2.371(6)	Ti1−C4	2.393(5)
Ti1−C5	2.404(5)	Ti1−Se1	2.5327(11)
Se1−Ti1−Se1a	92.93(5)	C6−Se1−Ti1	107.41(18)

[a] Symmetry operation: $a = y, x, -z$.

Table 3. Selected Bond Lengths [Å] and Angles [deg] for $[Cp_2Hf(SeMe)_2]$[a]

Hf1−C1	2.476(5)	Hf1−C2	2.492(4)
Hf1−C3	2.506(4)	Hf1−C4	2.500(5)
Hf1−C5	2.458(4)	Hf1−Se1	2.6113(5)
Se1−C6	1.963(5)		
Se1−Hf1−Se1a	96.24(2)	C6−Se1−Hf1	105.37(15)

[a] Symmetry operation: $a = y, x, -z$.

Table 4. Selected Bond Lengths [Å] and Angles [deg] for $[\{Cp_2Zr(SeMe)\}_2(\mu\text{-}O)]$

Zr1−O1	1.9675(16)	Zr1−Se1	2.6645(5)
Zr2−O1	1.9585(16)	Zr2−Se2	2.6689(5)
Se1−C11	1.967(3)	Se2−C22	1.965(3)
Zr−C	2.493(2)−2.564(2)		
O1−Zr1−Se1	101.14(5)	O1−Zr2−Se2	101.60(5)
C11−Se1−Zr1	109.05(9)	C22−Se2−Zr2	108.70(8)
Zr2−O1−Zr1	173.92(9)		

calculated positions and using the default C−H distance. Selected bond lengths and angles are given in Tables 2–4 with crystallographic data in Table 5.

Deposition Studies. LPCVD experiments were carried out in evacuated (10^{-1} mmHg) Pyrex (500 °C) or silica tubes (9 mm i.d.) with flat fused silica tile substrates (ca. 1 × 5 × 25 mm) that had previously been cleaned with acetone and demineralized water and dried at 100 °C overnight. The precursor (ca. 0.1 g) was loaded into the end of the tube, and this was positioned in a tube furnace such that the precursor sublimed slowly over the tiles in the hot zone. The precursor sublimed cleanly at this pressure over a period of 30−60 min with very little residue. A thermocouple placed inside a silica tube in a similar position to the precursor indicated the sublimation temperature to be approx 100 °C. The tube furnace was cooled, and the tube was transferred to the glovebox before removing the tiles for storage and characterization. Films were sputtered with a thin layer of carbon (EDX) or gold (imaging) and examined in a Jeol JSM5910 scanning electron microscope (SEM) with an Oxford Inca 300 energy dispersive X-ray microanalysis (EDX) probe. Powder X-ray diffraction (PXD) studies were carried out using a Bruker C2 Gadds diffractometer using Cu $K\alpha_1$ radiation, a fixed incident angle of 5°, and a 2θ range of typically 24−55°. XPS spectra were recorded using a Scienta ESCA300 spectrometer with a monochromated Al Kα X-ray source.

Table 5. Crystallographic Parameters[a]

complex	$[Cp_2Ti(SeMe)_2]$	$[Cp_2Hf(SeMe)_2]$	$[\{Cp_2Zr(SeMe)\}_2(\mu\text{-}O)]$
chemical formula	$C_{12}H_{16}Se_2Ti$	$C_{12}H_{16}HfSe_2$	$C_{22}H_{26}OSe_2Zr_2$
fw	366.07	496.66	646.79
crystal system	tetragonal	tetragonal	triclinic
space group	$P4_12_12$ (No. 92)	$P4_12_12$ (No. 92)	$P\bar{1}$ (No. 2)
a (Å)	9.3965(15)	9.5191(10)	8.2833(10)
b (Å)	9.3965(15)	9.5191(10)	10.763(2)
c (Å)	14.412(2)	14.604(2)	13.944(3)
α (deg)	90	90	69.034(10)
β (deg)	90	90	86.054(10)
γ (deg)	90	90	68.558(10)
V (Å^3)	1272.5(3)	1323.3(3)	1077.7(3)
Z	4	4	2
μ(Mo Kα) (mm^{-1})	6.359	13.351	4.354
total no. reflns.	9731	9940	28777
no. unique reflns.	1473	1525	6312
R_{int}	0.071	0.051	0.040
no. of parameters	70	69	244
$R1$ $[I_0 > 2\sigma(I_0)]$	0.042	0.020	0.027
$wR2$ $[I_0 > 2\sigma(I_0)]$	0.075	0.044	0.066
$R1$ [all data]	0.053	0.021	0.035
w$R2$ [all data]	0.079	0.045	0.069

[a] $R1 = \sum||F_o| - |F_c||/\sum|F_o|$. $wR2 = [\sum w(F_o^2 - F_c^2)^2/\sum wF_o^4]^{1/2}$.

Results and Discussion

Precursor Syntheses. The in situ insertion of Se into RLi (R = Me or Bu^t) in "frozen THF" solution,[16] followed by the slow addition to $[Cp_2MCl_2]$ (M = Ti, Zr or Hf) in anhydrous toluene, gives the complexes $[Cp_2M(SeR)_2]$ in moderate yield. The products are intensely yellow/orange colored solids and are extremely moisture sensitive; hence, samples were handled and stored in a glovebox (<1 ppm H_2O). The identities of the complexes were confirmed by ^1H, $^{13}C\{^1H\}$, and $^{77}Se\{^1H\}$ NMR spectroscopy, by microanalysis, and from crystal structures of representative examples. The corresponding tellurolate complexes $[Cp_2M(TeBu^t)_2]$ (M = Zr or Hf) were prepared using a similar approach but maintaining the reaction solution at −78 °C to prevent decomposition. The tellurolate complexes are deep red/orange solids which degrade over time even when stored in the glovebox. Solutions of these compounds are even less stable; hence, all spectroscopic measurements were made using freshly prepared solutions. Owing to the instability of the complexes we were unable to obtain satisfactory microanalyses for these; however, spectroscopic data parallel those in the selenolates. These are the first isolated tellurolate complexes of their type involving alkyltellurolates. Arnold and co-workers have shown that $[Cp_2Zr\{TeC(SiMe_3)_3\}_2]$ forms in situ at low temperature (−60 °C) but could not be isolated as it undergoes elimination of Te at around −20 °C in solution.[17] Aryl tellurolates such as $[Cp_2M(TePh)_2]$ and $[Cp_2M(o\text{-}C_6H_4Te_2)]$ (M = Ti, Zr or Hf)[18] and the bulky silyltellurolates $[Cp_2M\{TeSi(SiMe_3)_3\}_2]$ (M = Ti or Zr) represent the only related tellurolate complexes.[17] Attempts to prepare the corresponding $[Cp_2Ti(TeBu^t)_2]$ using a similar

(16) Gulliver, D. J.; Hope, E. G.; Levason, W.; Murray, S. G.; Potter, D. M.; Marshall, G. L. *J. Chem. Soc., Perkin Trans. II* **1984**, 429–434.
(17) Christou, V.; Wuller, S. P.; Arnold, J. *J. Am. Chem. Soc.* **1993**, *115*, 10545–10552.
(18) (a) Sato, M.; Yoshida, T. *J. Organomet. Chem.* **1974**, *67*, 395–399. (b) Meunier, P.; Gautheron, B.; Mazouz, A. *J. Organomet. Chem.* **1987**, *320*, C39–C43.

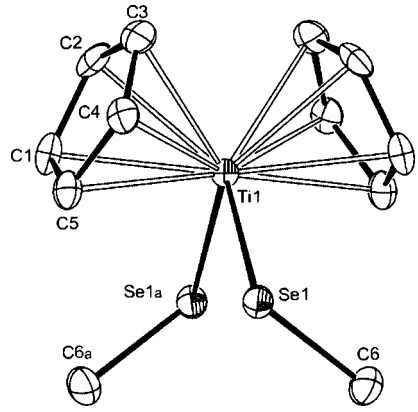

Figure 1. View of the structure of $[Cp_2Ti(SeMe)_2]$ with numbering scheme adopted. Ellipsoids are shown at the 50% probability level, and H atoms are omitted for clarity. Symmetry operation: $a = y, x, -z$.

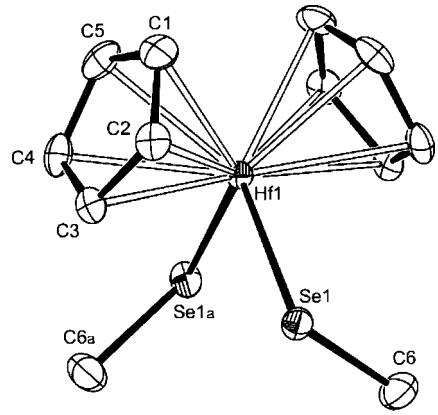

Figure 2. View of the structure of $[Cp_2Hf(SeMe)_2]$ with numbering scheme adopted. Ellipsoids are shown at the 50% probability level, and H atoms are omitted for clarity. Symmetry operation: $a = y, x, -z$.

method failed, with addition of the $LiTeBu^t$ solution leading to reduction to a dark blue Ti(III) species.

To confirm the successful synthesis of the complexes X-ray quality crystals of $[Cp_2Ti(SeMe)_2]$ and $[Cp_2Hf(SeMe)_2]$ were grown from solutions of the complexes in CH_2Cl_2/hexanes and cold Et_2O, respectively. The molecular structures are shown in Figures 1 and 2, and selected bond lengths and angles described in Tables 2 and 3, respectively. The structures show the metal ion coordinated to two η^5-Cp rings and two SeR^- ligands, giving pseudo-tetrahedral monomers. The M−Se bond distances are 2.5327(11) (Ti) and 2.6113(5) Å (Hf). The angles between the two $SeMe^-$ ligands are 92.93(5)° (M = Ti) and 96.24(2)° (Hf). The angles at Se, M−Se−C, are 107.41(18) (Ti) and 105.37(15)° (Hf).

Weakly diffracting crystals of $[Cp_2Ti(SeBu^t)_2]$ were obtained from a solution of the complex in cold Et_2O. The poor crystal quality led to rather weak data and higher than usual residuals (also hampered by disorder in the *t*-butyl substituents). However, the structure [formula $C_{18}H_{28}Se_2Ti$, molecular weight = 450.22, monoclinic, space group *C*2/*c*, a = 16.434(4), b = 9.3217(17), c = 12.668(2) Å, β = 108.391(15)°, V = 1841.5(6) Å^3, Z = 4, μ = 4.410 mm^{-1}, 2088 unique reflections, 94 parameters, R1 ($F > 4\sigma(F)$) = 0.086, wR2 ($F > 4\sigma(F)$) = 0 0.178] (Figure 4) is analogous to the methylselenolate complexes above, with pseudo-

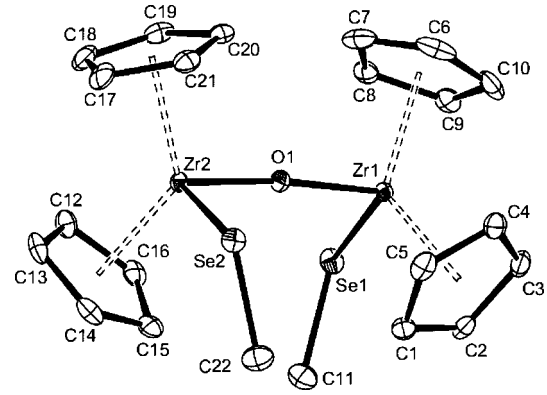

Figure 3. View of the structure of $[\{Cp_2Zr(SeMe)\}_2(\mu\text{-O})]$ with numbering scheme adopted. Ellipsoids are shown at the 50% probability level, and H atoms are omitted for clarity.

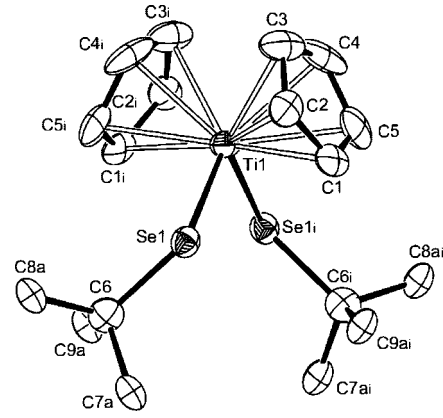

Figure 4. View of the structure of $[Cp_2Ti(SeBu^t)_2]$ with numbering scheme adopted. Ellipsoids are shown at the 35% probability level, and H atoms are omitted for clarity. There are two disordered orientations of the t-butyl group (a and b): only C7a, C8a, and C9a are shown. Symmetry operation: $i = -x, y, 1/2 - z$. Selected bond lengths and angles: Ti1−Se1 = 2.542(2), Se1−C6 = 2.005(13) Å, Se1−Ti1−Se1i = 99.14(11), and C6−Se1−Ti1 = 120.5(4)°.

tetrahedral Ti coordinated to the two Cp rings and to two terminal $SeBu^t$ ligands.

Analysis of the $^{13}C\{^1H\}$ NMR spectra for these complexes shows that while δ(Cp) (and $\delta(C_{quaternary})$ in the Bu^t complexes) are insensitive to the nature of the metal, δ(Me) in the $[Cp_2M(SeMe)_2]$ species shows significant dependence, shifting progressively to lower frequency along the series Ti → Zr → Hf. $^{77}Se\{^1H\}$ and $^{125}Te\{^1H\}$ NMR spectra were also obtained readily for these very soluble complexes in anhydrous chlorocarbon solution. Since the ^{77}Se and ^{125}Te NMR shifts in the alkali metal selenolate and tellurolate salts are expected to be highly solvent dependent, to compare the chemical shifts for the Group 4 complexes with the LiER species we also recorded $^{77}Se\{^1H\}$ and $^{125}Te\{^1H\}$ NMR spectra for solutions of the LiER salts in THF solution. Singlet resonances were observed for each of the LiER salts and for the $[Cp_2M(ER)_2]$ complexes, with very substantial high frequency shifts (Table 1) of several hundred ppm compared to the LiER salts. The trend in $\delta(^{77}Se)$ and $\delta(^{125}Te)$ with Group 4 metal follows the expected pattern, shifting to lower frequency from Ti → Zr → Hf, in line with the trend in the $\delta^{13}C$(Me) discussed above. However, the very large high frequency shifts observed for these chalcogenolate complexes compare with coordination shifts of a few tens

of ppm typically observed in selenoether (SeR_2) complexes with similar metals (there are no telluroether complexes of these elements).[19] This is consistent with a much increased donation of electron density from the chalcogen atom to the transition metal in the case of the ER^- ligand complexes, $\pi(E) \rightarrow M$ bonding being significant in the chalcogenolate complexes (cf. the chalcogenoethers which are regarded as modest σ-donor ligands with negligible π-bonding).

As expected, traces of water lead to rapid hydrolysis of the $[Cp_2M(ER)_2]$ complexes. Crystals were grown of the complex produced from a partially hydrolyzed solution of $[Cp_2Zr(SeMe)_2]$ in CH_2Cl_2. The structure shows (Figure 3, Table 4) an oxo-bridged dimeric species, $[\{Cp_2Zr(SeMe)\}_2(\mu\text{-O})]$, in which each Zr atom is coordinated to two η^5-Cp rings, one terminal $SeMe^-$ ligand, and the bridging oxo atom, providing a pseudotetrahedral coordination environment at each metal. The $Cp_2Zr(SeMe)$ fragments are in a staggered conformation, with the angle between the planes defined by Se(1)−Zr(1)−Zr(2) and Se(2)−Zr(1)−Zr(2) being 46.6°. A plausible mechanism for its formation is the hydrolysis of one of the Zr−Se bonds to form MeSeH and the reactive intermediate $[Cp_2Zr(SeMe)OH]$, which then reacts with a second molecule of $[Cp_2Zr(SeMe)_2]$ to form the oxo-bridged dimer. The Zr−Se bond distances (∼2.66 Å) are slightly longer than in the $[Cp_2Hf(SeMe)_2]$ above and 2.651(3) Å in $[Cp_2Zr(SePh)_2]$,[20] presumably due to the presence of an oxo ligand compared to a second selenolate. The Zr−O bond distances are ∼1.96 Å, similar to that in the related thiolate species $[\{Cp_2Zr(SPh)\}_2(\mu\text{-O})]$ (1.966(5) Å),[21] and the Zr−O−Zr unit is almost linear (173.92(9)°), consistent with significant $\pi(O) \rightarrow Zr$ bonding. Spectroscopic characterization of this oxo-bridged selenolate dimer was also undertaken so that its presence could be readily identified if formed in solutions of the bis-selenolate complex. The $\delta(^{77}Se) = 192.0$ for this dimer compares with 449.5 ppm for $[Cp_2Zr(SeMe)_2]$, reflecting the sensitivity of the Se atoms to the different electronic environment produced upon substituting one $SeMe^-$ ligand on each Zr atom for a bridging oxo ligand. The much lower $\delta(^{77}Se)$ NMR chemical shift observed in the oxo species suggests less $\pi(Se) \rightarrow Zr$ bonding in this complex compared to the bis-selenolate species, consistent with $\pi(O) \rightarrow Zr$ bonding being a significant component in the former (as implied from the structural data).

Deposition Studies. We reasoned that the mononuclear complexes formed via coordination of selenolate or tellurolate ligands to the well-defined Cp_2M fragment might give relatively volatile species suitable as precursors for ME_2 thin film deposition via LPCVD. This was especially of interest for ZrE_2 and HfE_2 films, which have not been obtained previously by CVD methods. Deposition experiments were carried out on the molecular $[Cp_2M(EBu^t)_2]$ (M = Ti, Zr, Hf) complexes due to the expected easier fragmentation of the E-C bonds in these compared to those containing the SeMe moiety. LPCVD was carried out at 450, 500, and 600 °C at a pressure of approximately 0.05 mbar.

Table 6. PXD Data for Metal Selenide Films Produced by LPCVD

sample	*a*, Å	*c*, Å
$TiSe_2$ 450 °C	3.562(10)	6.07(3)
$TiSe_2$ 500 °C	3.562(7)	6.05(3)
$TiSe_2$ 600 °C	3.569(7)	6.09(3)
bulk $TiSe_2$[24]	3.536−3.548	5.998−6.008
$ZrSe_2$ 450 °C	amorphous	
$ZrSe_2$ 500 °C[a]	3.788(18)	6.18(4)
$ZrSe_2$ 600 °C	3.797(3)	6.184(8)
bulk $ZrSe_2$[24]	3.798	6.192
$HfSe_2$ 450 °C	amorphous	
$HfSe_2$ 500 °C	3.760(5)	6.217(16)
$HfSe_2$ 600 °C	3.767(3)	6.197(11)
bulk $HfSe_2$	Unknown	

[a] Film was poorly diffracting.

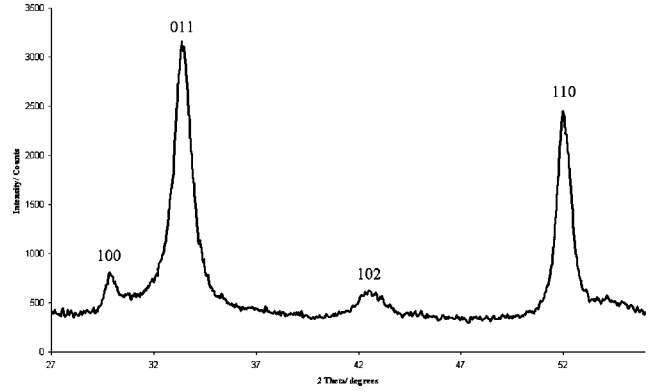

Figure 5. PXD pattern of $TiSe_2$ obtained at 600 °C. Reflections consistent with $TiSe_2$ are indicated by Miller indices.

All films were initially examined by PXD. When crystalline, they were found in all cases to exhibit the 1T structure ($P\bar{3}m1$, CdI_2 type). This is the normal structure type for $TiSe_2$ and $ZrSe_2$. For $HfSe_2$ no structure has been reported, but the 2H structure type (different layer stacking with a doubled, ∼12 Å, *c*-axis) is known for $Hf_{1.35}Se_2$.[22] Lattice parameters are listed in Table 6.[23] For the titanium selenide (Figure 5) and zirconium selenide films the lattice parameters closely matched the literature values for the bulk materials. For $TiSe_2$ these values are also very similar to those reported for films grown by single source LPCVD or dual source APCVD using selenoether precursors.[9,24] The lattice parameters found for $HfSe_2$ films (Figure 6) were similar to those of $ZrSe_2$ as would be expected from the similar ionic radii of Zr^{4+} and Hf^{4+}(0.72 and 0.71 Å, respectively).[25]

The SEM micrographs for the $TiSe_2$ films are displayed in Figure 7. At 450 °C a regular coating of small hexagonal platelets was observed, which grew with faces perpendicular to the silica surface as is common in these layered materials.[5–10] The platelets were around 1 μm across, an order of magnitude smaller than previously reported $TiSe_2$ films deposited by CVD from $TiCl_4$/selenoether combinations.[9,24] At 500 °C the tile was more densely covered with

(19) Levason, W.; Orchard, S. D.; Reid, G. *Coord. Chem. Rev.* **2002**, *225*, 159–199.
(20) Howard, W. A.; Trnka, T. M.; Parkin, G. *Inorg. Chem.* **1995**, *34*, 5900–5909.
(21) Yam, V. W.-W.; Qi, G.-Z.; Cheung, K.-K. *J. Organomet. Chem.* **1997**, *548*, 289–294.
(22) Shewe-Miller, I. M.; Young, V. G., Jr *J. Alloys Cmpds.* **1994**, *216*, 113–115.
(23) *PCPDFWIN*, version 2.4; Powder Diffraction File; International Center for Diffraction Data: Swarthmore, PA, 2003.
(24) Boscher, N. D.; Carmalt, C. J.; Parkin, I. P. *Chem. Vap. Deposition* **2006**, *12*, 54–58.
(25) Shannon, R. D. *Acta Crystallogr., Sect. A* **1976**, *32*, 751–767.

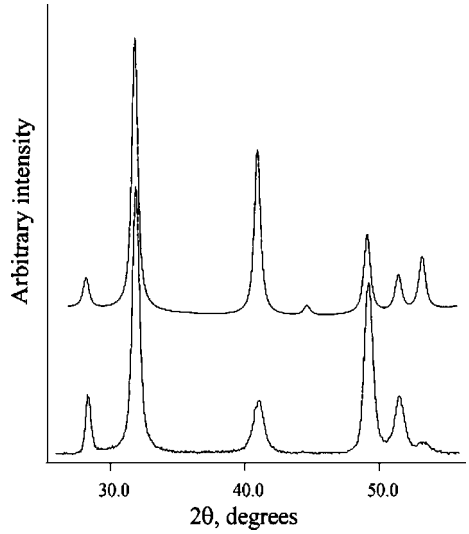

Figure 6. PXD pattern of $HfSe_2$: top calculated for $HfSe_2$ with atom positions set as for $ZrSe_2$; bottom, experimental pattern recorded on a film deposited at 600 °C.

crystallites of similar size that again grew perpendicular to the silica substrate. In this case, further growth of clusters of crystallites from the original layer is observed resulting in a "bubbled" surface, and presumably the existing crystals act as nucleation sites. At 600 °C the morphology changes, and irregular block shaped crystallites were observed.

LPCVD of $[Cp_2Zr(SeBu^t)_2]$ at 450 °C resulted in an amorphous pale green film on tiles at the entrance of the tube furnace, with no material deposited on the other tiles. At 500 °C a poorly diffracting dark green film was observed. SEM revealed the same plate morphology in this film as was observed for $TiSe_2$ at 450 and 500 °C. The hexagonal platelets grew perpendicular to the silica surface and had dimensions of less than 1 μm in the $a-b$ plane. At 600 °C a dark green crystalline film was obtained. SEM (Figure 8) reveals very small platelet crystallites ($\sim$0.2 μm) growing in a rope-like morphology. This growth mode appears to be intermediate between the two seen for $TiSe_2$, in that large numbers of much smaller crystallites form but the hexagonal platelet crystal habit is retained. It may be that $TiSe_2$ crystallites at 600 °C are less well formed because nucleation occurs easily at the higher temperature, and the precursor is highly volatile so it sublimes quickly ($[Cp_2Ti(SeBu^t)_2]$ is expected to be more volatile than $[Cp_2Zr(SeBu^t)_2]$ based on molecular weight).

Using $[Cp_2Hf(SeBu^t)_2]$ in LPCVD at 450 °C, only amorphous pale green films were observed. At 500 °C a dark blue film was deposited. SEM again revealed that the film grows as hexagonal platelets perpendicular to the substrate surface, with dimensions in the $a-b$ plane of approximately 0.5 μm. Carrying out the deposition at 600 °C formed a dark blue film. In contrast to $TiSe_2$ and $ZrSe_2$ deposited at 600 °C, well formed hexagonal platelets with around 0.5 μm diameter are observed (Figure 8). Again, the change is consistent with lower precursor volatility and slower growth. The formation of clusters of crystallites onto the initial layer, as seen for $TiSe_2$ at 500 °C, is seen in these micrographs.

EDX measurements on the $TiSe_2$ film obtained at 500 °C revealed a Ti:Se ratio of 1:1.7. A flat surface is required for good analysis, so these are nonideal samples, but this technique should give an indication of composition. XPS measurements on a $TiSe_2$ film obtained at 500 °C revealed Ti $2p_{3/2}$ = 456.3 and Ti $2p_{1/2}$ = 462.4 eV. Se $3d_{5/2}$ and $3d_{3/2}$ were observed at 53.9 and 54.7 eV, respectively, all relative to an adventitious carbon peak (285 eV). Ti $2p_{3/2}$, 459.3, and Se 3d, 53.2 eV, have been previously recorded for $TiSe_2$ prepared by dual source APCVD, although the authors note that the surface may be oxidized.[24] A Ti:Se ratio of 1:1.7 was obtained at the surface. Ar^+ ion etching resulted in a reduction in the Se content, presumably due to selective

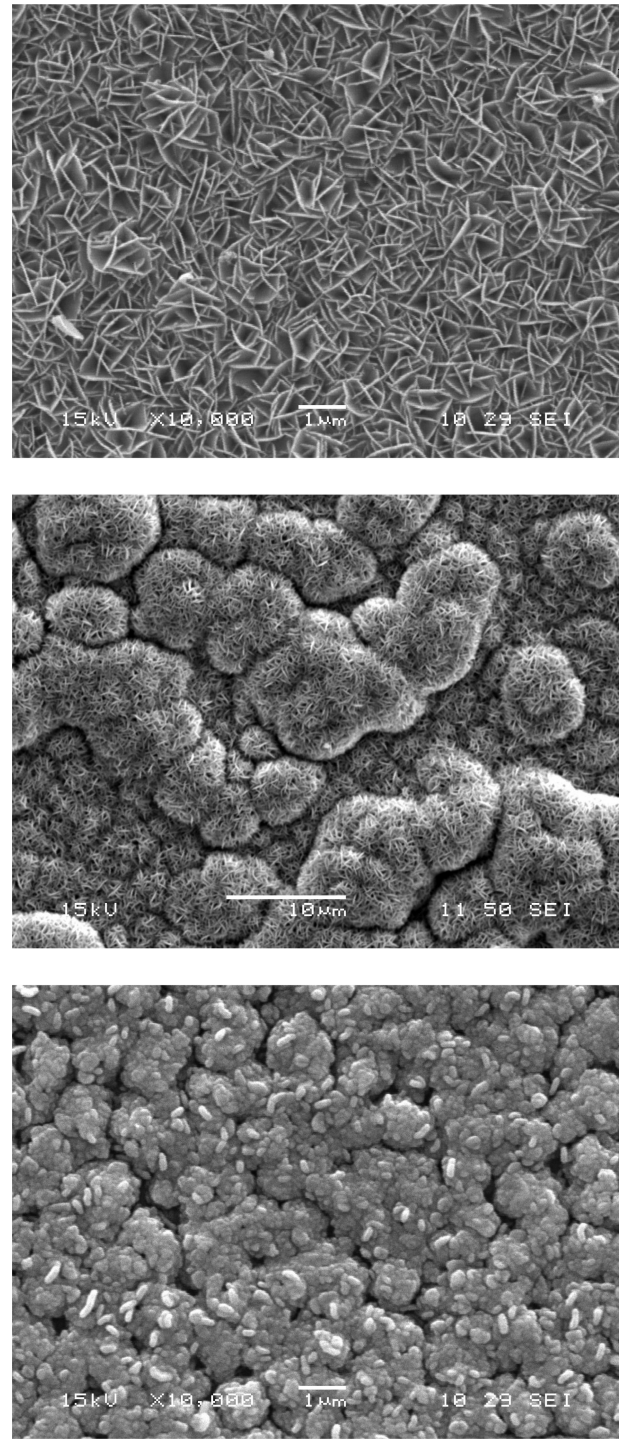

Figure 7. SEM micrographs of $TiSe_2$ deposited at 450 °C (top), 500 °C (middle), and 600 °C (bottom).

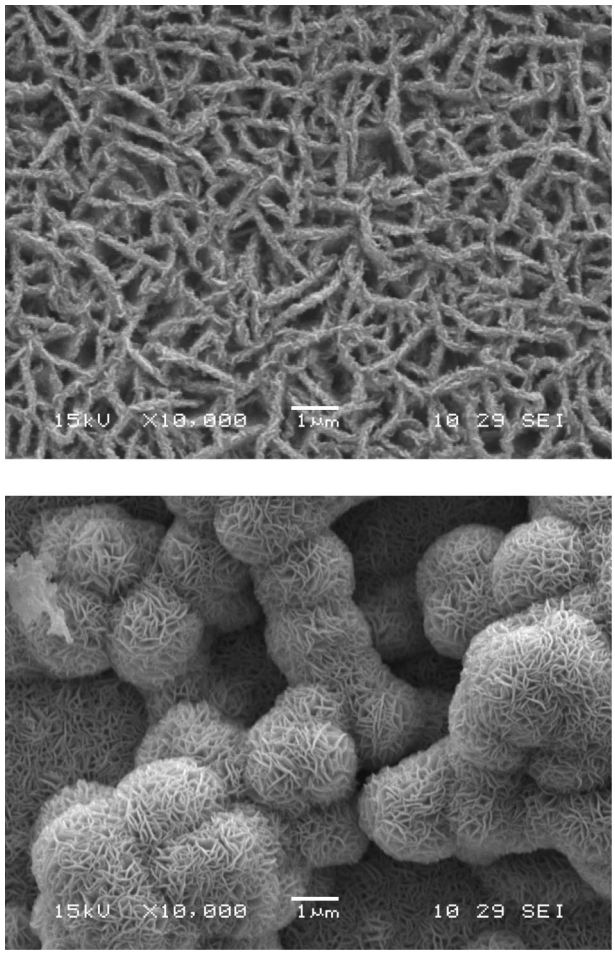

Figure 8. SEM micrographs of $ZrSe_2$ (top) and $HfSe_2$ (bottom) deposited at 600 °C.

etching. While both imperfect measurements, the same composition is obtained from EDX and XPS suggesting the films probably are Se deficient with composition close to $TiSe_{1.7}$. XPS indicated a carbon content of 15% by weight, and a small amount of oxygen was also observed (see comments below concerning air sensitivity). In the $ZrSe_2$ and $HfSe_2$ films, EDX measurements revealed a Zr:Se ratio of 1:1.5 and a Hf:Se ratio of 1:2.

XPS analysis of films that had been exposed to air during PXD measurements (i.e., for 2−3 h) showed significant surface oxidation with oxygen contents typically around 20 wt %. PXD measurements of the same films indicated no bulk structural change. The $TiSe_2$ film used for the analysis described earlier was exposed to air for a much shorter period (as it was inserted into the analysis chamber), and some oxygen was observed even after this short exposure. XPS only measures photoelectrons generated within 5 nm or less of the surface, and clearly on this length scale the sensitivity to oxygen or more likely moisture is severe. Samples kept in air for several weeks changed color and become amorphous.

Attempts to prepare MTe_2 films from the $[Cp_2M(TeBu^t)_2]$ complexes under similar conditions and at temperatures of 450 and 600 °C were unsuccessful. PXD and EDX analyses revealed the deposition only of gray elemental Te. This may be attributed to the weakness of the Te−alkyl bonds which leads to facile Te elimination from the complexes when heated in vacuo rather than sublimation (as required for LPCVD).

Conclusions

A series of chalcogenolate complexes of the form $[Cp_2M(ER)_2]$ (M = Ti, Zr or Hf; E = Se or Te; R = Me or Bu^t) has been prepared and characterized spectroscopically and in several cases crystallographically. The tellurolate complexes are the first isolated examples of their type involving alkyltellurolate ligands. Selenium-77 and tellurium-125 NMR spectroscopic studies reveal extremely large high frequency coordination shifts for these compounds, with a very significant dependence both upon the metal ion and the chalcogen type, indicating very substantial electron donation from the chalcogen to the transition metal center in the species. The $[Cp_2M(SeBu^t)_2]$ (M = Ti, Zr or Hf) complexes have been shown to be suitable as single source precursors for the deposition of MSe_2 by LPCVD, facilitating generation of all three Group 4 metal diselenides as intensely colored thin films with the 1T (CdI_2-type) structure. These are the first examples of deposition of $ZrSe_2$ or $HfSe_2$ by CVD from a single source precursor, and the first structural characterization of $HfSe_2$. The corresponding tellurolate complexes $[Cp_2M(TeBu^t)_2]$ (M = Zr or Hf) did not give MTe_2, probably due to the weak Te−alkyl bond leading to fragmentation of the parent complex with elimination of elemental Te. Work is ongoing to form complexes with more robust Te−C bonds and to investigate alternative ancillary ligands in the precursor complexes to allow MTe_2 thin film deposition.

Acknowledgment. We thank the EPSRC for supporting this work under EP/C001176/1 and for access to the NCESS XPS service funded under EP/E025722/1 and also the Royal Society for award of a University Research Fellowship to A.L.H. We also thank Professor I. P. Parkin and Dr. C. J. Carmalt (University College London) for helpful discussions.

Supporting Information Available: Crystallographic data (CIF). This material is available free of charge via the Internet at http://pubs.acs.org. These date have been deposited with the Cambridge Crystallographic Data Centre as supplementary publication numbers CCDC-670750 (Ti/Me), CCDC-750751 (Hf/Me), CCDC-670752 (Zr_2/Me), CCDC-750753 (Ti/Bu^t), and CCDC-750754 (Zr/Bu^t). The last structure is similar to the preceding t-butyl compound and is not discussed in the paper. These data can be obtained free of charge from the Cambridge Crystallographic Data Centre via www.ccdc.cam.ac.uk/data_request/cif.

CM800802G